Int. J. Electrochem. Sci., 14 **(2019)** 9755 – 9773, doi: 10.20964/2019.10.27

International Journal of
ELECTROCHEMICAL
SCIENCE
www.electrochemsci.org

Adiponitrile as a Novel Electrolyte Additive for High-Voltage Lithium-Ion Batteries

Liuyang Zhao[1], Shilei Bian[1], Zhicheng Ju[1], Yongli Cui[1], Yanhua Cui[2], Yueli Shi[1,], Quanchao Zhuang[1,*]*

[1] Li-ion Batteries Lab, School of Materials Science and Engineering, China University of Mining & Technology, Xuzhou 221116, China
[2] Institute of Electronic Engineering China Academy of Engineering Physics, Mianyang, 621000, P. R. China
[*]E-mail: zwysyl@163.com

Received: 25 June 2019 / *Accepted:* 10 August 2019 / *Published:* 30 August 2019

In his study, we reported adiponitrile (ADN) as a novel electrolyte additive for the $LiNi_{1/3}Co_{1/3}Mn_{1/3}O_2$ cathode electrode in voltage ranges of 3.0-4.4 V, 3.0-4.6 V and 3.0-4.8 V. The electrochemical properties of the electrodes were investigated by linear sweep voltammetry (LSV), a charge/discharge test, electrochemical impedance spectroscopy (EIS) and X-ray photoelectron spectroscopy (XPS). The results of this study showed that adding ADN to the electrolyte could effectively enhance the reversible capacity and cycling performance of the cathode electrode. The initial discharge capacities were 167.8 mAh g^{-1} and 214.8 mAh g^{-1} in electrolytes without and with 3% ADN, respectively. And the capacity retention rates were 68.4% and 70.4% at a voltage range of 3.0-4.6 V after 100 cycles in electrolytes without and with 3% ADN, respectively. The electrochemical performance was improved because of the compact and smooth solid electrolyte interface (SEI) film, which lowered the impedance between the cathode and the electrolyte by suppressing the decomposition of $LiPF_6$ and improving the stability of EC. In addition, adding 3%ADN to the electrolyte was favourable for obtaining a lower R_{ct}, which could promote the charge-transfer process by suppressing the interfacial reaction between the electrode and electrolyte.

Keywords: ADN; Lithium-ion batteries; Electrochemical properties; Electrochemical impedance spectroscopy

1. INTRODUCTION

Lithium-ion batteries are frequently used in portable electronic devices due to their long cycle life, sufficient energy density, outstanding cycle performance and stable working voltage [1-3]. However, it is still difficult to meet the robust power requirements of electric vehicles (EVs), hybrid electric vehicles (HEVs) and plug-in hybrid electric vehicles (PHEVs). Therefore, lithium ion batteries

need better electrochemical performance. One of the most effective ways to increase the energy densities of LIBs is to develop electrode materials with a high reversible capacity at high voltages [4, 5].

A large number of batteries are used to meet the standard voltage, and the number of batteries is determined by the voltage of a single battery. Therefore, increasing the voltage of a single battery can effectively reduce the number of batteries in series, thus simplifying the control circuit and promoting the overall reliability and safety of the battery pack. The development of high-voltage LIBs is largely determined by the operating voltage of the cathode electrode materials.

Layered transition-metal oxides, such as $LiNi_{1/3}Co_{1/3}Mn_{1/3}O_2$, have been frequently applied as cathode electrode materials due to their lower cost, higher capacity, better thermal stability and lower toxicity [6, 7].

Numerous studies have shown that high-voltage LIBs are severely restricted because the EC-based electrolyte easily decomposes at high voltages [8-10], and $LiPF_6$ decomposes when it encounters water. Moreover, the solid electrolyte interface (SEI) film and the cathode is corroded by HF, one of the decomposition products of $LiPF_6$ [10]. There are two methods to strengthen the stability of the electrolyte at high voltages: studying new types of electrolyte and searching for high voltage additives. Many studies have proven that electrolyte additives contribute to the effective stability of electrolytes and the formation of high quality SEI films [11,12]. SEI films can be composed of organic and inorganic compositions, but not all compositions are suitable for SEI films [13].

The SEI film can be modified by additives. Until now, additives such as fluorinated, ionic liquid, sulfone and nitrile solvents have been considered promising new high voltage solvents or co-solvents due to wide electrochemical stability windows and high oxidation potential. However, it is difficult and costly to synthesize fluorinated solvents [14]. For ionic liquid solvents, they have limited applications because of their low conductivity, high viscosity and poor wettability of the electrode [15]. The sulfone solvents have a melting point of 25°C, and the low-temperature and high rate performance of LIBs are limited by the relatively high viscosity and low conductivity of the sulfone solvents [6, 16].

However, nitrile compounds are considered promising high-voltage solvents owing to their unique properties. First, nitrile compounds possess high flash points and wide electrochemical stability windows(vs. Li/Li^+) [16-20]. Second, they have a positive effect on the interface between the electrode and electrolyte to improve the electrochemical performance [16][21]. According to previous reports, 3-methoxypropionitrile not only reduces the poor interfacial reaction between the solvent and the electrode but also accelerates desolvation of Li^+ ions, which was favourable for promoting the charge-transfer process [21-23].

So far, nitriles such as succinonitrile (SN), pimelonitrile (PN), glutaronitrile (GLN) and adiponitrile(ADN) show good thermal and high voltage stability.

According to previous reports, ADN can improve electrolyte stability because it can react with residual acids and water in the electrolyte to form amides. The reduction potential of ADN is lower than that of carbonate solvents, and ADN has a stronger electron donating ability, which may result in the formation of an SEI film that reduces impedance on the surface of the cathode material [24]. In addition, the median lethal dose (LD_{50}) value of ADN is 155 mg kg^{-1}, which is 31 times less toxic than potassium cyanide(KCN) (LD_{50}~5) [24, 25].

We herein introduce 3% ADN as an additive in the $LiPF_6$-EC:EMC=3:7 electrolyte for the $LiNi_{1/3}Co_{1/3}Mn_{1/3}O_2$ /Li half-cell. Fourier transform infrared (FTIR) spectroscopy was used to analyse the material structure. The specific capacity of the cells in the electrolyte without and with ADN was investigated using charge/discharge tests. Linear scan voltammetry (LSV) was used to measure the stability of the electrolyte without and with ADN. The morphology of the electrode was investigated using field emission scanning electron microscopy (FESEM). Electrochemical impedance spectroscopy (EIS) was applied to investigate the dynamic parameters during the process of lithium-ion insertion and extraction in the cathode electrode without and with ADN. The ion concentrations of the electrolytes were detected by laser ablation inductively coupled plasma mass spectrometry (LA-ICP-MS). According to the results of X-ray photoelectron spectroscopy (XPS), the modification of the solid electrolyte interface (SEI) film was realized by adding ADN.

2. EXPERIMENTAL

2.1 Preparation of the electrolytes

ADN was purchased from Shanghai Aladdin Biochemical Technology Co., Ltd. (China) and used without additional purification. The primary electrolyte was 1.0 M $LiPF_6$ in a mixture of ethylene carbonate (EC) and ethyl methyl carbonate (EMC) (3:7, wt.%, Xuzhou Zhaoda New Energy Technology Co. Ltd, China). The 1%, 2%, 3%, 4%, and 5% ADN (v/v) were added to the electrolyte in an argon-filled glove box (O_2 and H_2O content lower than 1 ppm) as the additive.

2.2 Preparation of the electrodes and cells

The $LiNi_{1/3}Co_{1/3}Mn_{1/3}O_2$ electrode used in this study was prepared by spreading a mixture consisting of 80 wt.% $LiNi_{1/3}Co_{1/3}Mn_{1/3}O_2$(provided by ATL. Inc., China), 3 wt.% carbon black, 7 wt.% graphite (Shanshan Limit Co., Shanghai, China) and 10% polyvinylidene fluoride(PVDF, HSV910, USA) binder dissolved in N-methyl-2-pyrrolidone (NMP, Aladdin Industrial Co. Ltd, Shanghai, China) onto an aluminium foil current collector. The foil was then cut into 1 cm^2 circle and 2×4 cm^2 rectangular plates as the electrodes for the half cell and the three-electrode cell, respectively [26]. The $LiNi_{1/3}Co_{1/3}Mn_{1/3}O_2$/Li coin-type half cells (2025) and three-electrode glass cells were assembled in an argon atmosphere glove box, and a Celgard 2400 was used as the battery separator in the coin-type half-cell.

2.3 Characterization

FTIR (Tensor-27, BRUKER) was carried out using a pellet containing a mixture of KBr in the range of 4000–650 cm^{-1}.

The charge/discharge performance of $LiNi_{1/3}Co_{1/3}Mn_{1/3}O_2$/Li coin-type half-cells was performed at room temperature by a battery analyser (Neware, Shenzhen, China) at a voltage range of

3.0-4.4 V, 3.0-4.6 V, and 3.0-4.8 V vs. Li/Li^+ at a constant current density of 50 mA g^{-1}.

The electrochemical windows of the electrolyte were measured by LSV using an electrochemical workstation (CHI 660C, Chenhua Co., Shanghai, China) at a scan rate of 0.2 mV s^{-1} at room temperature from an open circuit potential (OCP) of 3.7 V and 3.79 V to 6.0 V. The experiment was carried out in a three-electrode glass system in which the lithium foils were used as a reference electrode and a counter electrode, and a platinum wire was used as the working electrode.

The morphology of the electrode after the electrochemical tests in different electrolyte compositions was investigated by an LEO 1530 FE SEM (Oxford Instrument).

EIS measurements were performed in three-electrode cells, where Li foils were used as the counter and reference electrodes on an electrochemical workstation (CHI 660C, Chenhua Co., Shanghai, China). The amplitude of the ac perturbation signal was 5 mV, and the frequency varied from 10^5 to 10^{-2} Hz. The electrode was equilibrated for 1 hour before the EIS measurements. The impedance results obtained were fitted using Zview software.

The Ni, Co and Mn ion concentrations of the electrolytes were detected by LA-ICP-MS (NWR 213-7900 ICP-MS, ESI, Agilent, China). The 1 ml electrolyte samples, which had been tested by EIS and had been set aside for three days, were extracted and diluted before the ICP measurement.

To research the composition of the electrodes, the cells were disassembled in an Ar glove box after 10 cycles at a voltage range of 3.0-4.6 V. To remove the residual EC and $LiPF_6$, the cathode electrode was washed 3 times with DEC and then vacuum dried at 120°C for 12 hours to remove the residual DEC solvent. The elemental composition on the surface of the cathode was analysed by XPS (ESCALAB 250Xi, Thermo Fisher, USA).

3. RESULTS & DISCUSSION

3.1 Structure analysis of the ADN

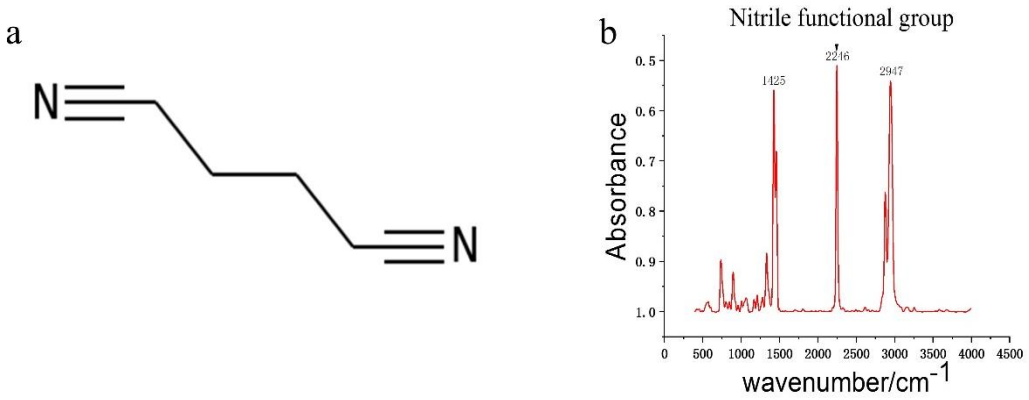

Figure 1. (a) Major structures of ADN and (b) FTIR spectra of the TP.

ADN is a colourless oily liquid. As shown in Figure 1(a), the adiponitrile in this experiment consists mainly of -CN functional groups. [22, 27] The feature peak of ADN in the FTIR spectra is

mostly at 3000–1400 cm^{-1}. Neat ADN showed a sharp single peak at 2246 cm^{-1} corresponding to the stretching mode of C≡N as shown in Fig. 1b. [28] Nitrile functional groups can react with water in acidic conditions (H^+), which reduces the decomposition of $LiPF_6$ into HF at the same time. [1, 27]

3.2 The charge/discharge test of the $LiNi_{1/3}Co_{1/3}Mn_{1/3}O_2$/Li coin-type half-cells.

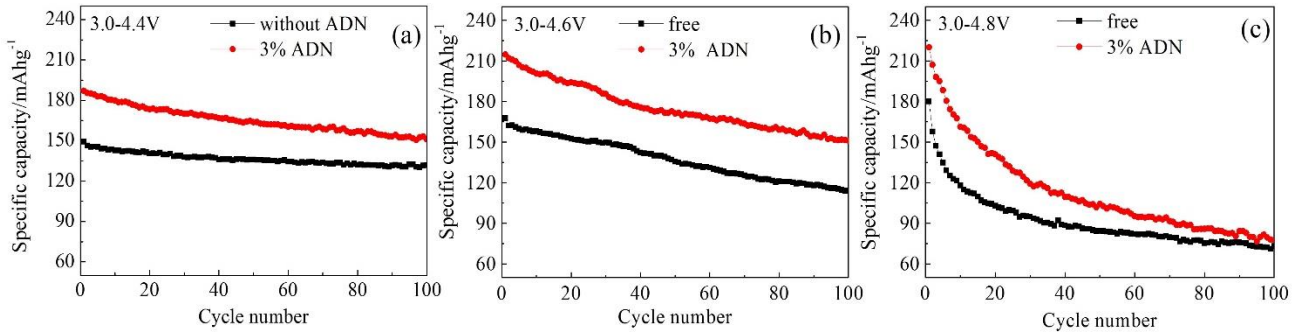

Figure 2. The cycle performance of $LiNi_{1/3}Co_{1/3}Mn_{1/3}O_2$/Li cells in the electrolyte without and with 3% ADN in the potential range of (a) 3.0-4.4 V, (b) 3.0-4.6 V and (c) 3.0-4.8 V.

The charge–discharge cycle curves of the $LiNi_{1/3}Co_{1/3}Mn_{1/3}O_2$/Li cells in the electrolytes without and with 1%, 2%, 3%, 4%, and 5% ADN (v/v) at 3.0-4.4 V, 3.0-4.6 V and 3.0-4.8 V were displayed in Fig. S1, Fig. S2, Fig. S3, Table S1, Table S2 and Table S3. The capacities of the $LiNi_{1/3}Co_{1/3}Mn_{1/3}O_2$/Li cells in the electrolytes with 3% ADN were always higher than those of the other electrolytes during the 100 cycles. Therefore, the following research focuses on the above electrode.

As shown in Fig. 2(a), the first discharge capacities of the cells in the electrolyte without and with 3% ADN were 149.2 mAh g^{-1} and 187.1 mAh g^{-1}, respectively, in the potential range of 3.0-4.4 V. The corresponding capacities were 131.9 mAh g^{-1} and 151.0 mAh g^{-1} after 100 cycles without and with 3% ADN, respectively.

As shown in Fig. 2(b), the first discharge capacities of the cells in the electrolyte without and with 3% ADN were 167.8 mAh g^{-1} and 214.8 mAh g^{-1}, respectively, in the potential range of 3.0-4.6 V. The corresponding capacities were 114.2 mAh g^{-1} and 151.2 mAh g^{-1} after 100 cycles without and with 3% ADN, respectively.

As shown in Fig. 2(c), the first discharge capacities of the cells in the electrolyte without and with 3% ADN are 180.2 mAh g^{-1} and 220.1 mAh g^{-1}, respectively, in the potential range of 3.0-4.8 V. The corresponding capacities are 73.3 and 77.8 mAh g^{-1} after 100 cycles without and with 3% ADN, respectively.

The above results indicated that ADN added to the electrolyte was beneficial for increasing the first capacity and the cycle capacity in different voltage ranges.

3.3 Electrochemical stability of ADN

The oxidation decomposition of the carbonate-based electrolytes at high voltage has greatly

restricted the development of high voltage LIBs. The electrochemical stability of the electrolyte without and with 3% ADN is shown in Fig. 3. The current densities increased significantly when the voltage was higher than 4.5 V and 4.7 V in the electrolyte without and with ADN, respectively. Therefore, the additive ADN could improve the stability of the electrolyte [29, 30].

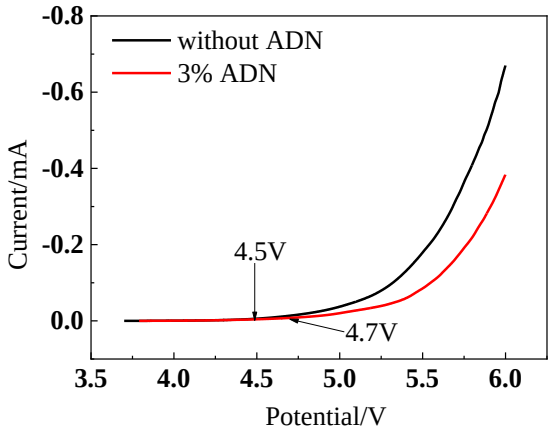

Figure 3. Linear sweep voltammograms of Pt electrodes in the electrolyte without and with 3% ADN electrolyte from an open circuit potential (OCP) of 3.7 V and 3.79 V to 6.0 V at 0.2 mV s^{-1}

3.4 Characterization of the $LiNi_{1/3}Co_{1/3}Mn_{1/3}O_2$ electrode surface

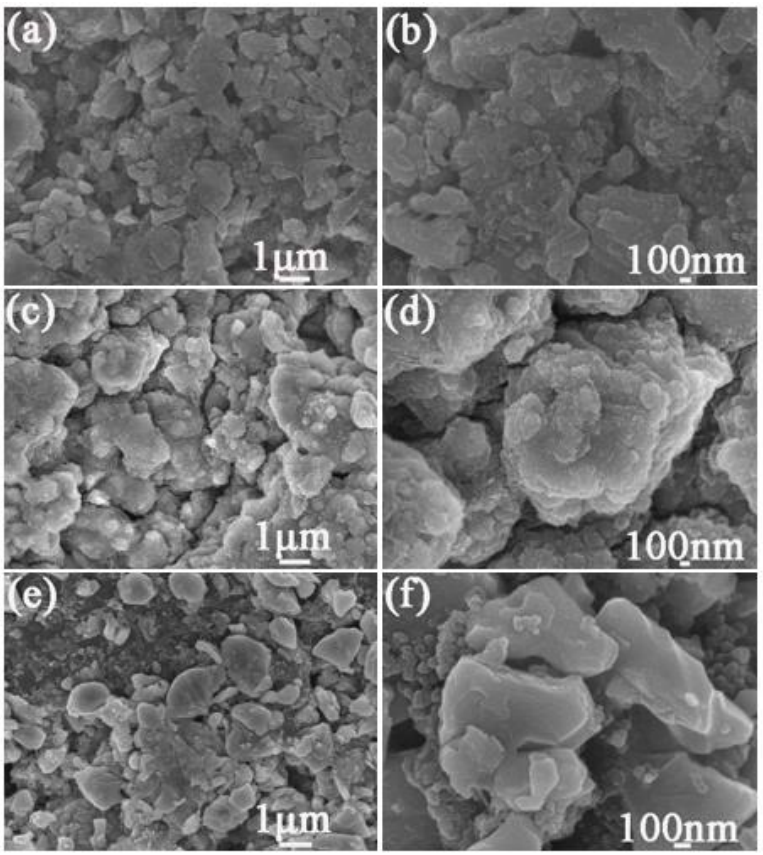

Figure 4. SEM micrographs of the $LiNi_{1/3}Co_{1/3}Mn_{1/3}O_2$ electrode: before cycling (a, b); after 100 cycles in the electrolyte without ADN; (c, d) after 100 cycles with 3% ADN; and (e, f) after 100 cycles.

To further probe the effects of additives on the $LiNi_{1/3}Co_{1/3}Mn_{1/3}O_2$ cathodes at 4.6 V, SEM analysis of the electrodes was performed before and after 100 cycles. The SEM micrographs of the $LiNi_{1/3}Co_{1/3}Mn_{1/3}O_2$ electrode before and after cycling in different electrolytes are shown in Fig. 4. As shown in Fig. 4 (a, b), there was no coverage found on the surface of the $LiNi_{1/3}Co_{1/3}Mn_{1/3}O_2$ cathode before the cycle. The morphology of the $LiNi_{1/3}Co_{1/3}Mn_{1/3}O_2$ electrode in the electrolyte without 3% ADN was covered with deposits, which showed serious agglomeration, as shown in Fig. 4 (c, d). However, compact and smooth SEI films could be observed on the electrodes in the electrolyte with 3% ADN, as shown in Fig. 4 (e, f).

3.5 EIS measurements

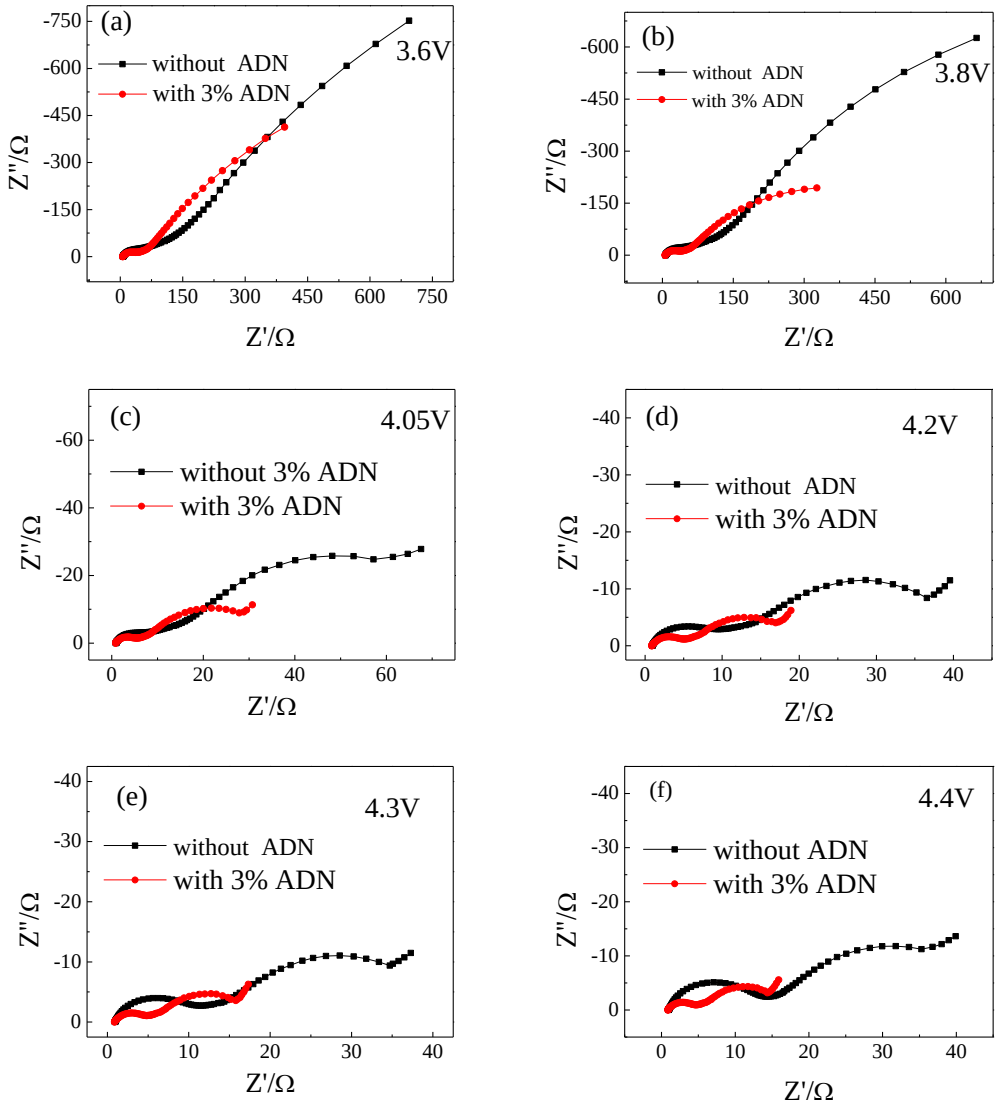

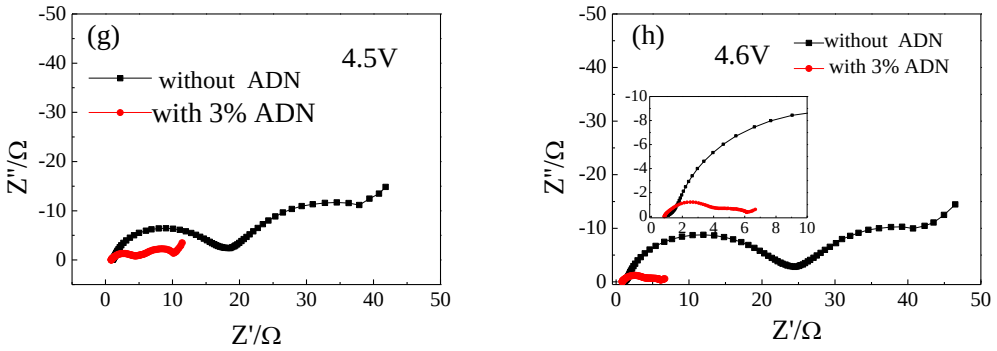

Figure 5. Nyquist plots (a-h) of the $LiNi_{1/3}Co_{1/3}Mn_{1/3}O_2$ electrode in the first charge process at various potentials from 3.6 V to 4.6 V in the electrolyte without and with 3% ADN

EIS has been extensively used in the study of electrode reaction mechanisms of LIBs in recent years [31-33]. The Nyquist plots of the $LiNi_{1/3}Co_{1/3}Mn_{1/3}O_2$ electrode in the first charge process at various potentials from 3.6 V to 4.6 V in the electrolyte without and with 3% ADN are shown in Fig. 5. The trends of the above Nyquist plots were similar. At the open circuit potential of 3.6 V, the Nyquist plots showed that there was a small semicircle in the high frequency region (abbreviated as HFS) and a slightly tilted line in the low frequency region (abbreviated LFL) [34-36]. When the potential increased to 4.05 V, the Nyquist graphs of the above two types consisted of 3 parts, namely, HFS, MFS (middle-frequency semicircle, abbreviated as MFS) and LFL. According to previous studies [37, 38], the LFL, MFS and HFS can be attributed to the solid state diffusion of lithium ions, the charge transfer step and the migration of lithium ions through the SEI film, respectively. It can be seen from the graph that the semicircles of the electrode in the electrolyte with 3% ADN were less throughout than that of the electrode in the electrolyte without ADN.

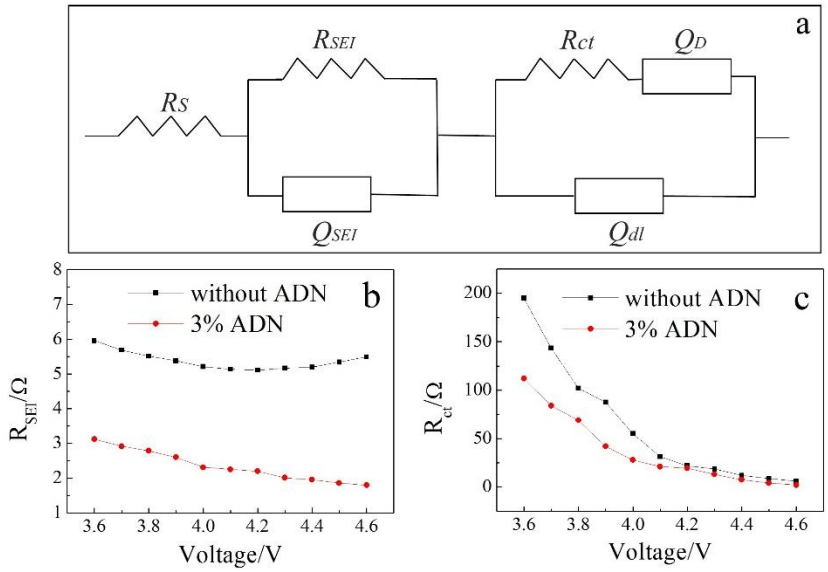

Figure 6. (a) Equivalent circuit proposed for fitting impedance spectra of the $LiNi_{1/3}Co_{1/3}Mn_{1/3}O_2$ electrode in the first charge process. Variations of (b) R_{SEI} and (c) R_{ct} with the electrode potential in electrolytes without and with 3% ADN.

Based on the above analysis, to adapt to the impedance spectrum of the $LiNi_{1/3}Co_{1/3}Mn_{1/3}O_2$ electrode during the first charge process, an equivalent circuit was proposed, as shown in Fig. 6(a)[39, 40]. In this equivalent circuit, R_{ct} represents the resistance of the charge transfer reaction, R_s represents the ohmic resistance, and R_{SEI} represents the resistance of the SEI film. The double layer and the capacitances of the SEI film are represented by the constant phase elements (CPEs) Q_{dl} and Q_{SEI}, respectively[26]. Considering that the low frequency region could not be modelled properly using the finite Warburg element, we used a CPE instead, i.e., Q_D. The Q_D CPE is a component used to characterize the nonideal behaviour of the electrode, and the expression for the admittance response of the CPE (Q) is:

$$Y = Y_0\omega^n \cos(\frac{n\pi}{2}) + jY_0\omega^n \sin(\frac{n\pi}{2}) \quad (1)$$

where n stands for the dispersion coefficient, ω is the angular frequency and j is the imaginary unit. A capacitor with capacitance of C when n=1, a CPE represents a resistor when n=0, a Warburg resistance when n=0.5 and an inductor when n=-1.

Fig. 6(b) shows the variations of R_{SEI} obtained by simulating the experimental impedance spectra of the cathode electrode during the first lithium ion intercalation process in the electrolytes without and with 3% ADN. The R_{SEI} of the electrode in the electrolyte with 3% ADN was lower than that of the electrode in the electrolyte without ADN (Fig. 6(b)). In the electrolyte with 3% ADN, R_{SEI} decreased continuously from 3.6 V to 4.2 V. This phenomenon was commonly attributed to the reaction between the SEI film and electrolyte [41, 42]. However, when the potential increased from 4.2 V to 4.6 V, R_{SEI} in the electrolyte without 3% ADN increased with the increase of the electrolyte polarization potential, which may be attributed to the crack and repair of the SEI film at a high voltage. Nevertheless, in the electrolyte with 3% ADN, the R_{SEI} showed a downward trend from 3.6 V to 4.6 V. It could be seen that an ADN addition was beneficial for obtaining an SEI film with a lower R_{SEI}, especially at high voltages, and improved the stability of the electrolyte.

As shown in Fig. 6(c), R_{ct} has a similar tendency in both electrolytes. The R_{ct} in the electrolyte containing no additive is larger than the R_{ct} in the electrolyte with 3% ADN. This indicated that lithium ions were more easily intercalated into and deintercalated from the cathode electrode in the electrolyte with 3% ADN.

3.6 Ion concentration test

The Ni, Co and Mn ion concentrations in the electrolyte without and with 3% ADN after the EIS test are shown in Fig. 7. The concentrations of Ni, Co and Mn ions were 13.252 ppm, 14.948 ppm and 14.451 ppm in the electrolyte without ADN, respectively. In the electrolyte with 3% ADN, the Ni and Mn ion concentrations were 0.982 ppm and 0.305 ppm, respectively. Co could not be detected owing to a low content. Thus, the dissolution of the metal ions was effectively inhibited by adding 3% ADN to the electrolyte, indicating that the reaction between the electrodes and electrolytes was suppressed, which could obviously improve the capacity and cyclability of cells. The result was consistent with the charge/discharge test.

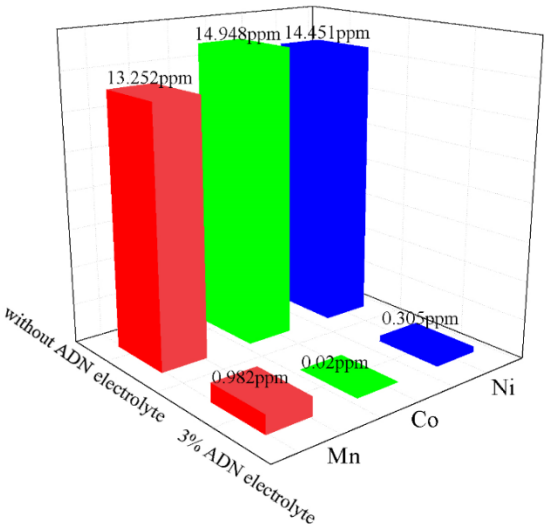

Figure 7. The Ni, Co and Mn ion concentrations in the electrolyte without and with 3% ADN after the EIS test

3.7 XPS of the $LiNi_{1/3}Co_{1/3}Mn_{1/3}O_2$ electrode.

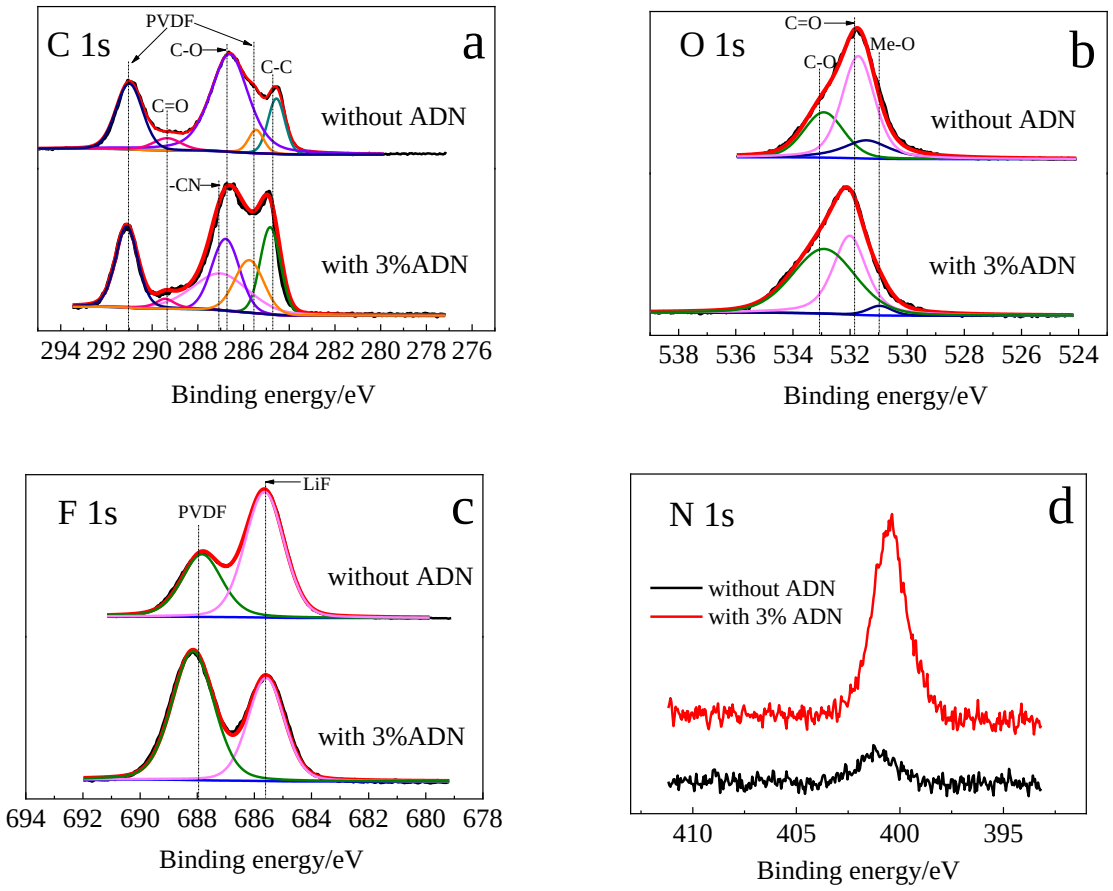

Figure 8. XPS spectra of $LiNi_{1/3}Co_{1/3}Mn_{1/3}O_2$ electrodes after 10 cycles in the electrolyte without and with 3% ADN.

Figure 8 (a, b, c, d) shows the XPS spectra of C 1s, O 1s, F 1s and N 1s of the $LiNi_{1/3}Co_{1/3}Mn_{1/3}O_2$ cathodes after 10 cycles of the charge/discharge test in the electrolyte without and with 3% ADN additive.

As displayed in Fig. 8(a), the peak near 291.1eV and 285.7eV of the C 1s in was attributed to the PVDF binder, while the peak near 289.4eV was related to the C=O bond; the peak near 286.7eV was attributed to the C-O bond, and the peak of 284.8eV was associated with the C-C bond, which indicated the presence of typical compositions of the surface in the above two cathodes, such as Li_2CO_3, Lithium alkoxides (ROLi), lithium carbonates ($ROCO_2Li$), and poly(ethylenecarbonate) (PEC) [43, 44]. Furthermore, the lower intensity of the peaks of C=O and C-O with 3% ADN indicated that unstable compositions such as Li_2CO_3 and the composition of poly(ethylenecarbonate) (PEC) (the oxidation product of EC) on the cathode surface were suppressed. The CN group (287 eV) from the C 1s spectra shown in Fig. 8(a) and the N 1s spectra (400 eV) shown in Fig. 8(d) [25] were only observed in the electrolyte with ADN, which indicated that the nitrogen present on the cathode surface was derived from the ADN additive.

As shown in Fig. 8(b), the O 1s spectra at 530.9 eV (Me-O), 532ev (C=O), and 532.9 eV (C-O) corresponded to the metal oxide, lithium alkoxides, and lithium carbonates and PEC, respectively [45]. The lower intensity of the peak (Me-O, 530.9 eV) in the electrolyte with 3% ADN demonstrated that ADN added in the electrolyte could effectively alleviate metal deposition on the cathode surface to a certain extent.

From Fig. 8(c), the peak of LiF (685.6 eV), one of the components of the SEI film, was relatively low in the 3% ADN electrolyte, indicating that the decomposition of $LiPF_6$ was inhibited to a certain extent by adding 3% ADN [46, 47].

4. CONCLUSION

ADN was investigated as a new and stable electrolyte additive for a $LiNi_{1/3}Co_{1/3}Mn_{1/3}O_2$ electrode at high voltage. The electrochemical performance of the cathode electrode in the voltage range of 3.0-4.4 V, 3.0-4.6 V and 3.0-4.8 V was improved in the electrolyte with 3% ADN.

These improvements were attributed to the following reasons. First, the compact and smooth SEI film with a lower impedance between the cathode and electrolyte was obtained by adding 3% ADN to the electrolyte. Second the decomposition of $LiPF_6$ was suppressed and the stability of EC was improved, especially in the voltage range from 4.2 V to 4.6 V. Third, adding 3% ADN to the electrolyte was favourable for obtaining a lower R_{ct}, which could promote the charge-transfer process by suppressing the interfacial reaction between the electrode and electrolyte.

ACKNOWLEDGMENTS
This work was supported by the Fundamental Research Funds for the China University of Mining and Technology (2017XKQY063).

References

1. R. Chen, L. Fan, C. Yan, Y. Ye, Y. Huang, W. Feng and L. Li, *J. Power Sources*, 306 (2016) 70.
2. S. J. Lei, X. D. Dong, G. M. Yuan, Y. X. Qian, C. Yong, H. X. Jing, Z.X. Dong, Y. Y. Xia, Y. X. Qing, G. Y. Guo, G. Lin and W. Li, *Adv. Mater.*, 30 (2018) 1705575.
3. Z. L. Min, Z. Kai, H. Zhe, T. Z. Liang, M. L. Qiang, K. Y. Mook, C. Lei and C. Jun, *Adv. Energy Mater.*, 8 (2018) 1701415.
4. Q. Su, Y. Li, L. Li, W. Li, G. Cao, L. Xue, J. Li and X. Cao, *Mater. Lett.*, 198 (2017) 180.
5. J. Cha, J. G. Han, J. H. Wang, J. Cho and N. S. Choi, *J. Power Sources*, 357 (2017) 97.
6. K. Xu, *Chem. Rev.*, 104 (2004) 4303.
7. Y. Cho, S. Lee, Y. Lee, T. Hong and J. Cho, *Adv. Energy Mater.*, 1 (2011) 821.
8. L. Xing, W. Li, C. Wang, F. Gu, M. Xu, C. Tan and J. Yi, *J. Phys. Chem. B.*, 113 (2009) 16596.
9. Y. Zhu, M. D. Casselman, Y. Li, A. Wei and D. P. Abraham, *J. Power Sources*, 246 (2014) 184.
10. M. Hu, X. Pang and Z. Zhou, *J. Power Sources*, 237 (2013) 229.
11. J. Q. Liu, Q. C. Zhuang, Y. L. Shi, X. Yan, X. Zhao and X. Chen, *RSC. Adv.*, 6 (2016) 42885.
12. J. Xia, L. Madec, L. Ma, L. D. Ellis, W. Qiu, K. J. Nelson, Z. Lu and J. R. Dahn, *J. Power Sources*, 295 (2015) 203.
13. S. S. Zhang, *J. Power Source*, 162 (2006) 1379.
14. Z. Zhang, L. Hu, H. Wu, W. Weng, M. Koh, P. C. Redfern, L. A. Curtiss and K. Amine, *Energy Environ. Sci.*, 6 (2013) 1806.
15. L. Hu, Z. Zhang and K. Amine, *Electrochem. Commun.*, 35 (2013) 76.
16. S. Li, D. Zhao, P. Wang, X. Cui and F. Tang, *Electrochim. Acta*, 222 (2016) 668.
17. Q. Wang, P. Pechy, S. M. Zakeeruddin, I. Exnar and M. Grätzel, *J. Power Sources*, 146 (2005) 813.
18. Q. Wang, S. M. Zakeeruddin, I. Exnar and M. Gratzel, *J. Electrochem. Soc.*, 151 (2004) A1598.
19. H. Duncan, N. Salem and Y. A. Lebdeh, *J. Power Sources*, 117 (2013) 25.
20. E. N. Maury, J. Świątowska, A. Chagnes, S. Zanna, P. T. Van, P. Marcus and M. Cassir, *Electrochim. Acta*, 115 (2014) 223.
21. Q. Wang, S. M. Zakeeruddin, I. Exnar and M. Grätzel, *J. Electrochem. Soc.*, 151 (2004) A1598.
22. Y. A. Lebdeh and I. Davidson, *J. Electrochem. Soc.*, 156 (2009) A60.
23. R. Chen, F. Liu, Y. Chen, Y. Ye, Y. Huang, F. Wu and L. Li, *J. Power Sources*, 306 (2016) 70.
24. X. Song, T. Meng, Y. Deng, A. Gao, J. Nan, D. Shu and F. Yi, *Electrochim. Acta*, 281 (2018) 370.
25. S. Li, D. Zhao, P. Wang, X. Cui and F. Tang, *Electrochim. Acta*, 222 (2016) 668.
26. Q. C. Zhuang, J. Li and L.L. Tian, *J. Power Sources*, 222 (2013) 177.
27. I. Ken, D. Pippel, S. Chmitz, W. Rippe and K. Unze, *Electrochim. Acta*, 56 (2011) 7530.
28. Y. A. Lebdeh and I. Davidson, *J. Power Sources*, 189 (2009) 576.
29. L. Jiang, L. Sheng, X. Chen, T. Wei and Z. Fan, *J. Mater. Chem. A.*, 4 (2016) 11388.
30. R. F. Li, S. Q. Wu, Y. Yang and Z. Z. Zhu, *J. Phys. Chem. C.*, 114 (2010) 16813.
31. N. Dimov, K. Fukuda, T. Umeno, S. Kugino and M. Yoshio, *J. Power Sources*, 114 (2003) 88.
32. Y. Q. Chu, Z. W. Fu and Q. Z. Qin, *Electrochim. Acta*, 49 (2004) 4915.
33. W. C. Choi, D. B. Yun, J. K. Lee and B. W. Cho, *Electrochim. Acta*, 50 (2004) 523.
34. X. Zhang, A. Mauger, Q. Lu, H. Groult, L. Perrigaud, F. Gendron and C. M. Julien, *Electrochim. Acta*, 55 (2010) 6440.
35. Y. S. Lee, K. S. Lee, Y. K. Sun, Y. M. Lee and D. W. Kim, *J. Power Sources*, 196 (2011) 6997.
36. C. X. Ding, Y. C. Bai, X. Y. Feng and C. H. Chen, *Solid State Ionics*, 189 (2011) 69.
37. D. P. Abraham, S. Kawauchi and D. W. Dees, *Electrochim. Acta*, 53 (2008) 2121.
38. A. Funabiki, M. Inaba and Z. Ogumi, *J. Power Sources*, 68 (1997) 227.
39. X. Y. Qiu, Q. C. Zhuang, Q. Q. Zhang, R. Cao, P.Z. Ying, Y. H. Qiang and S. G. Sun, *Phys. Chem. Chem. Phys.*, 14 (2012) 2617.
40. Q. C. Zhuang, J. Li and L. L. Tian, *J. Power Sources*, 222 (2013) 177.

41. D. Aurbach, K. Gamolsky, B. Markovsky, G. Salitra, Y. Gofer, U. Heider, R. Oesten and M. Schmidt, *J. Electrochem. Soc*., 147 (2000) 1322.
42. D. Ostrovskii, F. Ronci, B. Scrosati and P. Jacobsson, *J. Power Sources*, 103 (2001) 10.
43. S. H. Kang, D. P. Abraham, A. Xiao and B.L. Lucht, *J. Power Sources*, 175 (2008) 526.
44. L. Xia, Y. Xia and Z. Liu, *Electrochim. Acta*, 151 (2015) 429.
45. L. Yang, B. Ravdel and B. L. Lucht, *J. Electrochem. Soc.*, 13 (2010) A95.
46. J. H. Park, J. S. Kim, E. G. Shim, K. W. Park, Y. T. Hong, Y. S. Lee and S. Y. Lee, *Electrochem. Commun.*, 12 (2010) 1099.
47. S. Wilken, M. Treskow, J. Scheers, P. Johansson and P. Jacobsson, *RSC Adv*., 3 (2013) 16359.

SUPPORTING MATERIAL

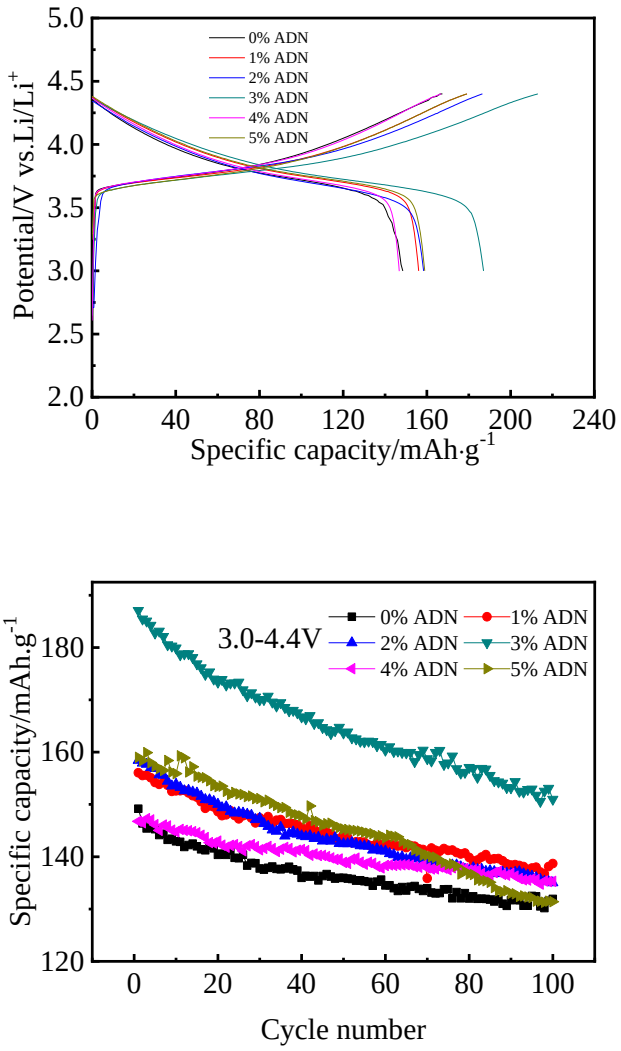

Figure S1 The first charge-discharge characteristics and cyclic performance of the $LiNi_{1/3}Co_{1/3}Mn_{1/3}O_2$ cathode with different concentrations of ADN additives in the voltage range of 3.0-4.4 V.

Table S1 The charge-discharge properties of the $LiNi_{1/3}Co_{1/3}Mn_{1/3}O_2$ electrode with different ratios of ADN additives added.

	0%ADN	1%ADN	2%ADN	3%ADN	4%ADN	5%ADN

Initial discharge capacity /mAh g^{-1}	148.2	156.1	158.4	187.1	146.8	159.0
Coulomb efficiency of first cycle /%	89.1	87.2	84.9	87.8	88.1	88.8
Capacity after 100 cycles/ mAh g^{-1}	131.9	138.7	135.0	151.0	135.3	131.4
Capacity retention /%	88.4	88.9	85.2	80.7	92.2	82.6

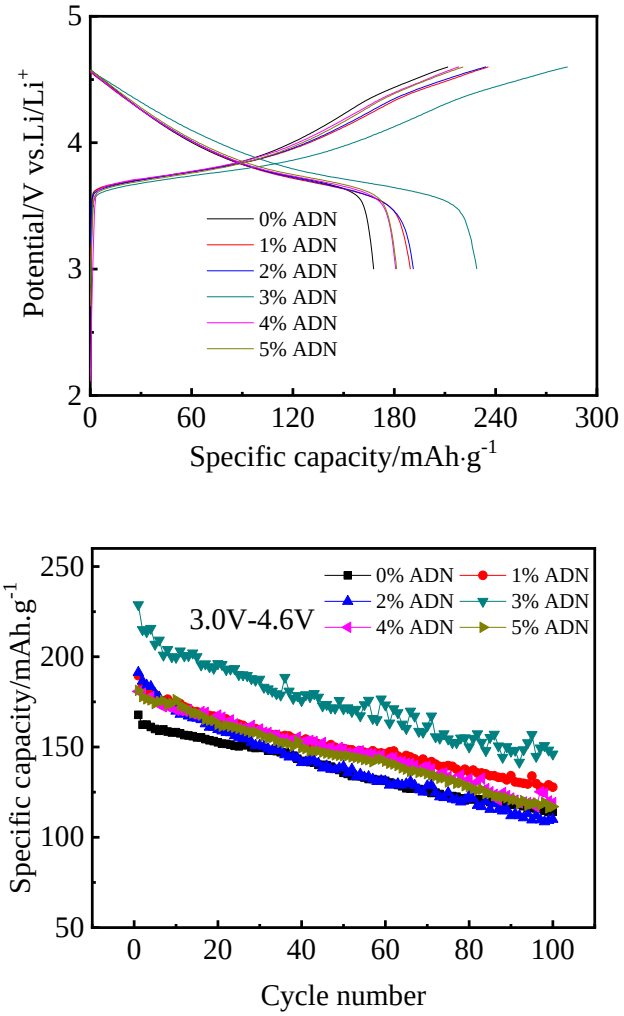

Figure S2 The first charge-discharge characteristics and cyclic performance of the $LiNi_{1/3}Co_{1/3}Mn_{1/3}O_2$ cathode with different concentrations of ADN additives in the voltage range of 3.0-4.6 V.

Table S2 The charge-discharge properties of the $LiNi_{1/3}Co_{1/3}Mn_{1/3}O_2$ electrode with different ratios of ADN additives added.

	0%ADN	1%ADN	2%ADN	3%ADN	4%ADN	5%ADN

Initial discharge capacity / mAh g^{-1}	167.8	189.5	191.3	228.8	180.8	181.4
Coulomb efficiency of first cycle /%	79.1	80.4	81.6	80.9	82.7	82.2
Capacity after 100 cycles /mAh g^{-1}	114.2	127.8	110	146.1	119.2	117
Capacity retention /%	68.1	67.4	57.5	63.9	65.9	64.5

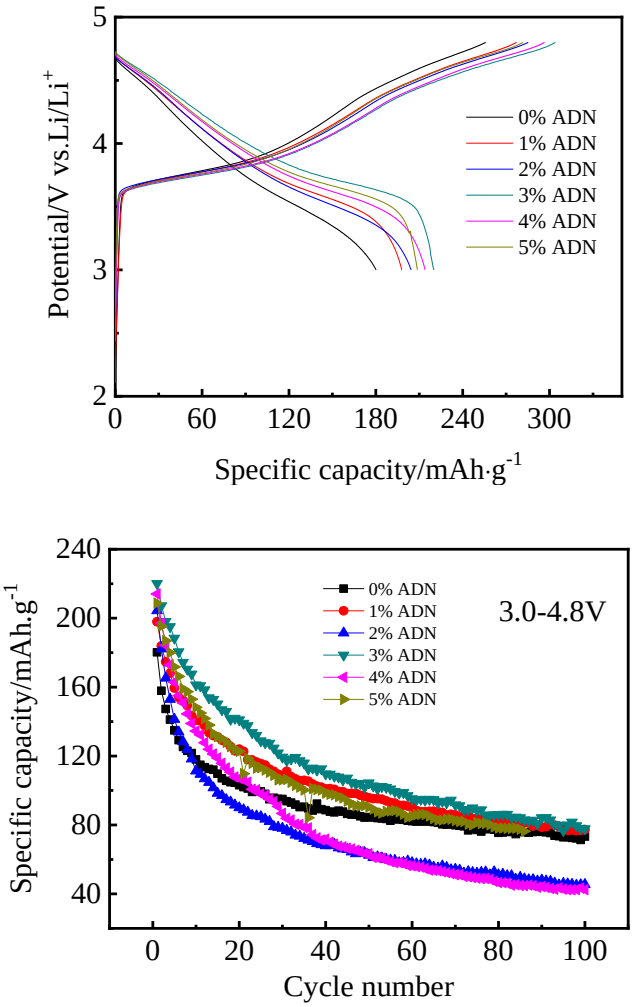

Figure S3 The first charge-discharge characteristics and cyclic performance of the $LiNi_{1/3}Co_{1/3}Mn_{1/3}O_2$ cathode with different concentrations of ADN additives in the voltage range of 3.0-4.8 V.

Table S3 The charge-discharge properties of $LiNi_{1/3}Co_{1/3}Mn_{1/3}O_2$ electrode with different ratios of ADN additives added.

	0%ADN	1%ADN	2%ADN	3%ADN	4%ADN	5%ADN

Initial discharge capacity / mAh g^{-1}	180.2	197.9	204.4	220.1	214.0	208.7
Coulomb efficiency of first cycle /%	70.4	71.4	71.7	72.4	72.2	74.1
capacity after 100 cycles /mAh g^{-1}	73.3	77.3	45.5	77.8	42.4	76.4
Capacity retention /%	40.7	39.1	22.3	35.3	19.8	36.6

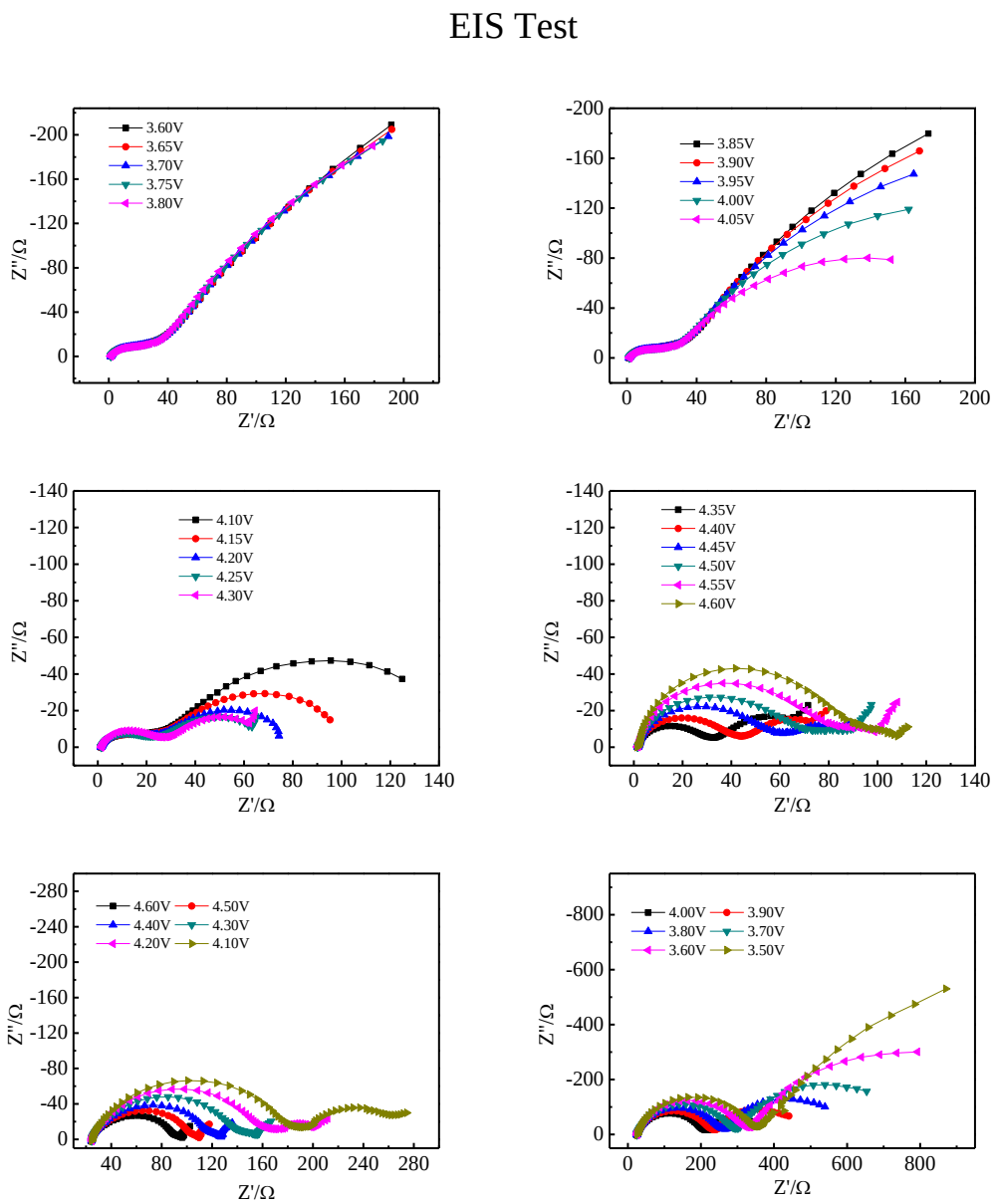

Figure S4 Nyquist plots of the $LiNi_{1/3}Co_{1/3}Mn_{1/3}O_2$ cathode during the first charge and the discharge process in electrolyte without ADN

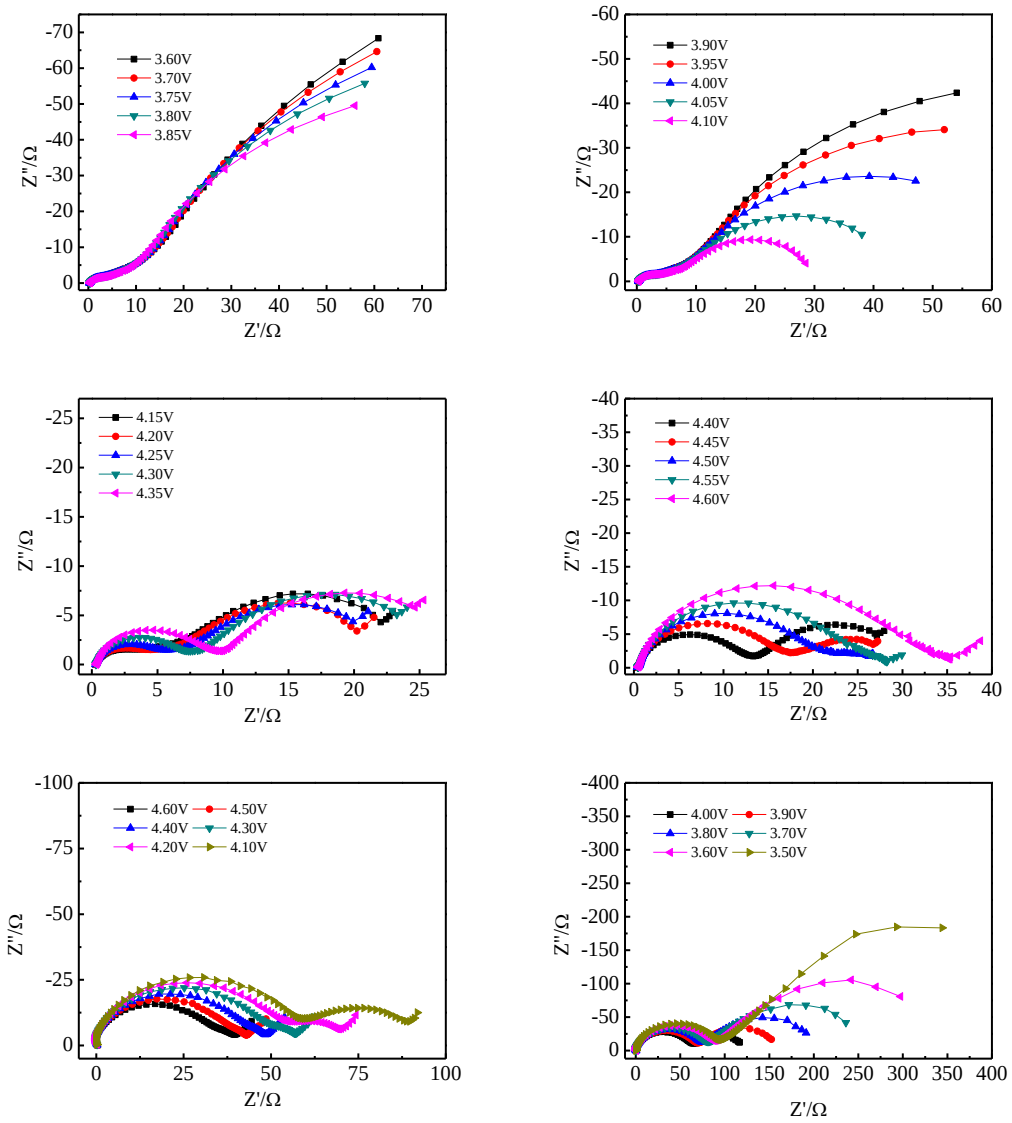

Figure S5 Nyquist plots of the $LiNi_{1/3}Co_{1/3}Mn_{1/3}O_2$ cathode during the first charge and the discharge process with a 3% ADN additive

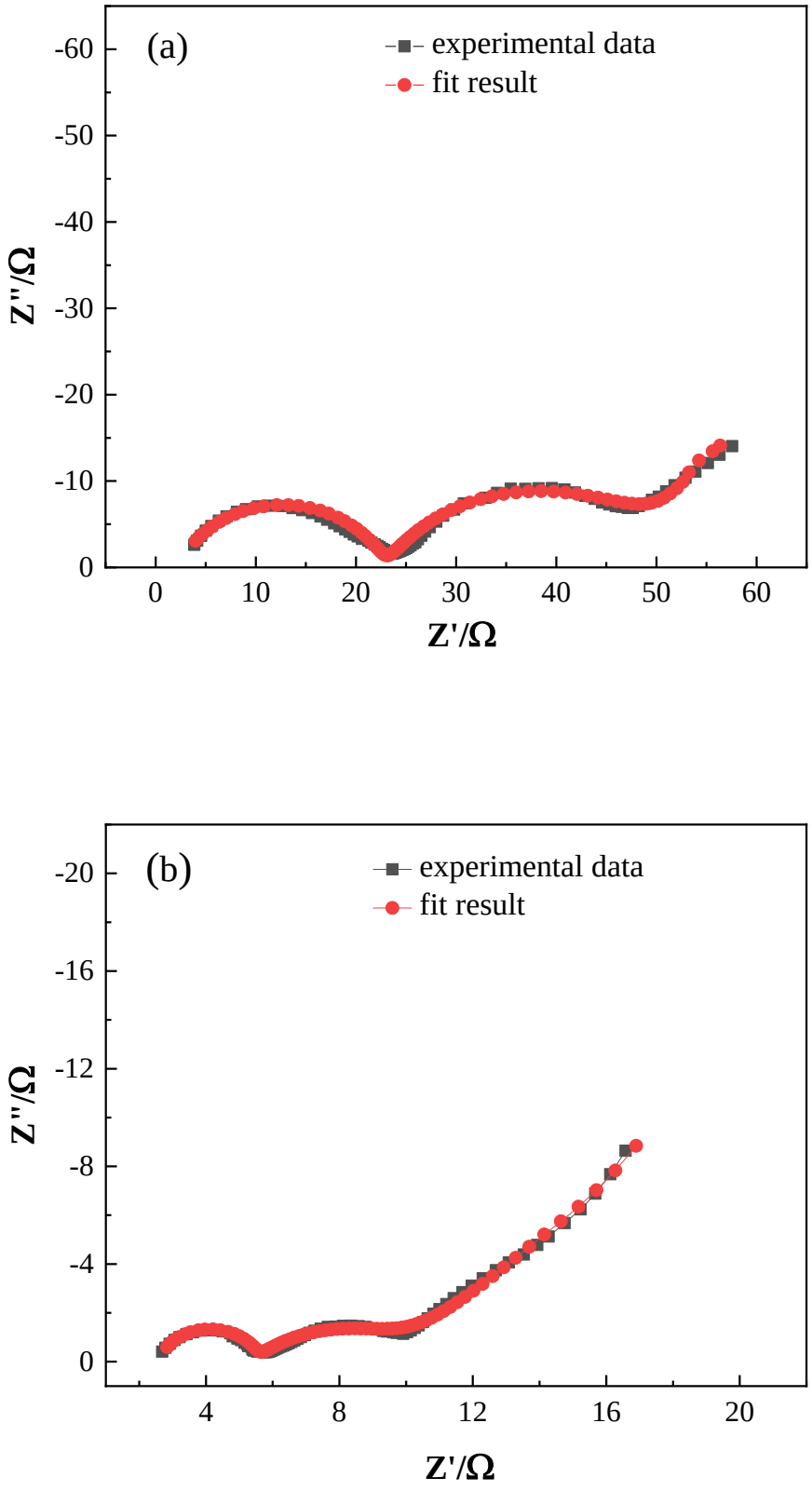

Figure S6 Comparison of the EIS data and fit result at 4.5 V (a) without ADN and (b) with 3% ADN

Table S4 Equivalent circuit parameters of the Nyquist fitting results in the first charge cycle at 4.5 V in the electrolyte without and with ADN

Parameters charge: 4.5 V	In the electrolyte without ADN		In the electrolyte with ADN	
	Value	Uncertainty (%)	Value	Uncertainty (%)
R_s (Ω)	2.248	5.0298	2.633	1.326
R_{SEI}(Ω)	5.57	1.0505	2.156	2.2532
Q_{SEI}-n	$8.9336*10^{-6}$	9.97037	$6.4007*10^{-6}$	18.007
Q_{SEI}-Y_o	0.77284	1.1741	0.93145	1.796
R_{ct} (Ω)	20.6	4.2983	16.857	4.859
Q_D-n	85.66	17.615	115.1	12.703
Q_D-Y_O	0.73043	8.5754	0.55367	2.6239
Q_{dl}-n	0.011533	5.8773	0.016788	11.256
Q_{dl}-Y_o	0.67966	2.9529	0.60301	3.8225